URSI GASS 2021, Rome, Italy, 28 August - 4 September 2021

Isolation of the Small-Scale and Weak Medium-Scale TIDs on Daytime Midlatitude Ionograms

Adel Akchurin*, Gregory Smirnov, and Vyacheslav Ildiryakov
Kazan Federal University, Russian Federation, 420008, https://kpfu.ru

Abstract

A simple indicator has been introduced to detect weak mid-latitude TIDs in ionograms. This indicator is based on the differential rotation of the cusp part of the trace of the F layer. This approach turned out to be much simpler than the analysis and isolation of various additional traces in the form of cusps and hooks. Such an approach turned out to be more capable for highly noisy ionograms. Processing of 3-month data allowed us to detect clear daily-seasonal variations in the intensity of SSTIDs in autumn observations.

1 Introduction

Researchers of weak mid-latitude travelling ionospheric disturbances (TIDs) currently have no other tool available except ionosondes, whose high sensitivity (dN/N > 3%) is provided by the total reflection of HF radio waves. The other methods of sounding the ionosphere actively used in mid-latitudes are inferior to sounding by decameter radio waves in terms of price/quality ratio. Thus, in the widely used TEC data on a dense grid of GNSS receivers it was difficult to approach the sensitivity dN/N ~ 10% in detecting medium-scale TIDs (MSTIDs) on TEC perturbation maps. This was possible only with careful selection of line-of-sight passing between the receiver and the GNSS satellite [1, 2]. Small-scale TIDs (SSTIDs), whose horizontal dimensions are less than 100 km, usually have a low intensity (dN/N < 10%), which makes them practically invisible for all remote methods operating at frequencies well above the critical frequencies of the mid-latitude ionosphere. An exception is the expensive incoherent scatter radars operating on the plasma line and, in fact, absent at mid-latitudes. Owing to such actual low observability of SSTIDs, their ionosonde measurements are very important.

It is known that in the family of TIDs the small-scale ones (horizontal dimensions less than ~100 km) are poorly understood due to the complexity of their detection. The complexity of their detection was due to their low dN/N intensity, which, on average, did not exceed 10%, making it impossible to observe them in widely used TEC data [1]. Except for daytime plasma line IS radars [3] and space-based measurements [4], the only detectors capable of long-term measurements are ionosondes with (quasi)vertical incidence. The only condition is a high rate of sounding not worse than 1 ionogram per minute, because the time of SSTIDs observation on the ionograms is from several minutes to 10.

The complexity of detecting disturbances with horizontal dimensions of less than 100 km and the absence of continuous measurements also created some confusion in the classification of such disturbances, which, as in [5], we attributed to SSTIDs. So, depending on the taste preferences of the authors, one can find works where heterogeneities of this scale are called large-scale irregularities [6], if the author considered them to be a product of a random/turbulent process, or disturbances of an intermediate scale [7], if the author saw them as the generation of internal gravitational waves rather than the product of random processes with the same spatial dimensions.

2 The choice of observation parameters of weak SSTIDs

On the ionograms of (quasi)vertical incidence, disturbances/heterogeneities with horizontal scales of less than 100 km appear as additional traces of the cusp- and hook-liked form [8]. For simplicity, we will use the short term cusp below. The typical movement of these cusps downward in frequency and height along the trace of the main layer F from its critical frequency to its beginning over a time interval of about 5-10 minutes is tempting to consider this period as the existence of the heterogeneity that generated the cusp in the ionogram, for example, assuming vertically descending disturbance/heterogeneity. However, the observational capabilities of the ionosonde do not allow the horizontal movement of a longer-lived inhomogeneity to be ruled out, which requires further investigation. Nevertheless, despite the uncertainty in the determination of both the lifetime and the occurrence frequency, we attribute these ionogram signatures to small-scale disturbances (rather than large-scale irregularities), because on ionograms, they are seen as a discrete event, progressively moving along the ionogram from sounding to sounding, as happens with the “classic” larger-scale TIDs.

The analysis of the appearance of the above cusps or SSTIDs was based on an indirect approach - the analysis of changes in the tail of the trace of the F layer (its cusp arc). Using the entire trace is inconvenient, since the main layer F itself may contain additional layering (for example, on F1 and F2). Such an approach in the analysis turned out to be more productive for us than trying to

isolate and understand all the many forms of the appearance of SSTIDs on ionograms [8]. The use of the cusp arc of the F layer as a proxy indicator of the SSTIDs turned out to be quite justified, since the appearance of cusps/hooks is almost always accompanied by a change in the shape of the cusp arc. To fix such changes, we introduced special parameters based on the selection of the differential rotation of the tail of the trace of the F layer, which turns its cusp arc at a critical frequency into a horizontal strip [9].

An example of such a differential rotation is shown in Figure 1. On the left side of the figure, the tail parts of the cusp arc of layer F are shown. Red shows the original cusp arc, green and orange show two examples of rotation of the trace points by a different angle $\alpha = A \times B^{C \times r}$ depending on the distance r from the center of rotation [9]. Using many of our ionograms, it was found that the parameters B and C can be constant and equal to 1.81 and 0.065, respectively. The final form for the angle of rotation of the points of the cusp arc was as follows $\alpha = 0.9 \times k \times 1{,}81^{0{,}065r}$, where the parameters for fitting are the parameter k and the position of the pivot center.

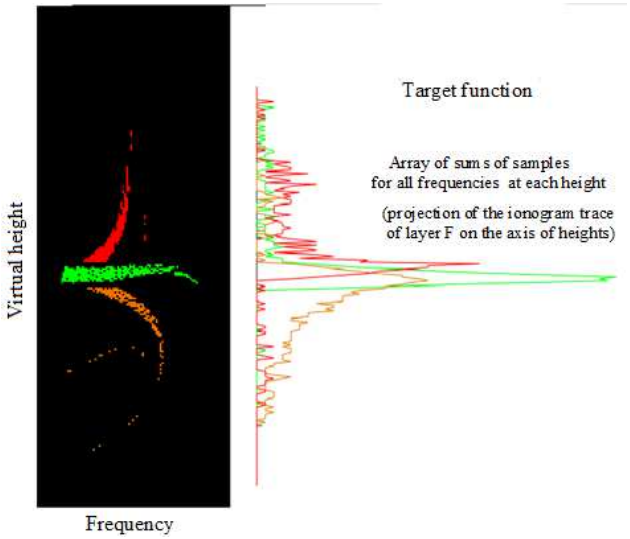

Figure 1. Determination of the optimal differential rotation of the tail of the extraordinary trace. On the left is a fragment of the ionogram with a cusp arc. Red markes the original cusp arc, green and yellow indicate two examples of differential rotation performed. Three examples of the target function for finding the optimal rotation are shown on the right. The color of the graphs of the target function correspond to the colors of the cusp arcs on the left side of the figure. The best fit results in the narrowest and highest target function.

It seems to us that the most successful position of the center of rotation could be the intersection point of the ordinary and extraordinary traces, since in this case almost the entire curved part of the cusp arc of the extraordinary trace would be captured. However, to simplify the processing, the point of an extraordinary trace at the critical frequency of an ordinary trace (*foF*2) is currently taken as the center of rotation. In this case, a small part of the cusp arc of the extraordinary trace is lost, but then there is no need to separate the ordinary and extraordinary traces. Subsequent analysis showed that this simplification does not lead to serious omissions in the detection of SSTIDs.

Thus, the search for the optimal differential rotation that turns the cusp arc into a flat horizontal segment reduces to fitting two parameters a degree of up-stretching/down-shrinking, $k_{US/DS}$, and a height of the extraordinary trace at the critical frequency of the ordinary trace or height of pivot center of differential rotation, h_{PC}. To clarify what these parameters reflect and how they can be better than the classical parameters of the critical frequency and layer height, Figure 2 shows an example of the typical behavior of an autumn daytime layer F during the passage of TID. Figure 2 shows four enlarged fragments from a series of ionograms containing the cusp portion of the main trace of layer F. As can be seen from the figure at 13:46, layer F was in a calm state, which we conventionally called flattened. As a weak perturbation passes, the trace of the F layer begins to stretch upward and decrease slightly in frequency (~0.2 MHz). This stretching reaches a maximum after 6 minutes, then the shrinking of the trace of the F layer down to the initial state, which is reached after 8 minutes, begins. At this last stage, an additional trace in the form of a cusp or hook may be observed. The differential rotation was introduced by us in order to enhance the effect of passing the TID when the critical frequency variations do not exceed 0.3 MHz.

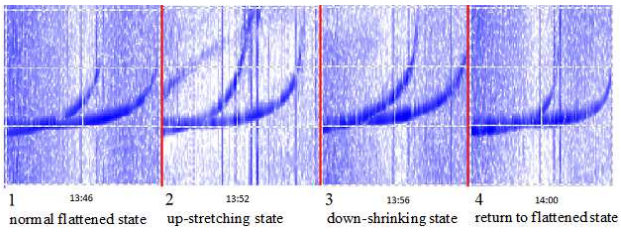

Figure 2. An example of typical behavior of the cusp portion of the main trace of layer F during the passage of a TID.

The diurnal variations of this parameter associated with the differential rotation made it possible to detect diurnal variations in the intensity of SSTIDs in autumn observations. Namely, in diurnal variations in the intensity of SSTIDs, approximately 2-hour periods of increased and decreased intensity are observed (or modulation of the intensity of SSTIDs). So for the entire autumn period, these 2-hour periods form bands approximately parallel to the position of the evening terminator. Interestingly, the low-intensity band takes a 2-hour time interval to the evening terminator. The parameters of the observed modulation of the intensity of the daytime mid-latitude SSTIDs of the geomagnetically quiet time are similar to the similar parameters recorded

by ionosondes [10] and incoherent scattering radars [11], [12] during the motion of the main ionospheric trough in geomagnetically disturbed periods .

Using the daytime variations of the above parameters ($k_{US/DS}$, h_{PC}) in the autumn period of 2018, a seasonal-diurnal pattern of the occurrence of MS and SSTIDs was collected, shown in Fig. 3. In this picture, approximately 2-hour periods of increased and decreased intensity (or modulation of the intensity of SSTID) were found, forming bands approximately parallel to the position of the evening terminator. These bands are shown in Fig. 3 with lines of white and violet colors, and also marked with numbers 1 and 2. Note that the slope of these lines corresponds to the superrotating (supercorotating) appearance of daytime TIDs, i.e. similar TIDs appear on ionograms on a given day 4-10 minutes earlier than on the previous day.

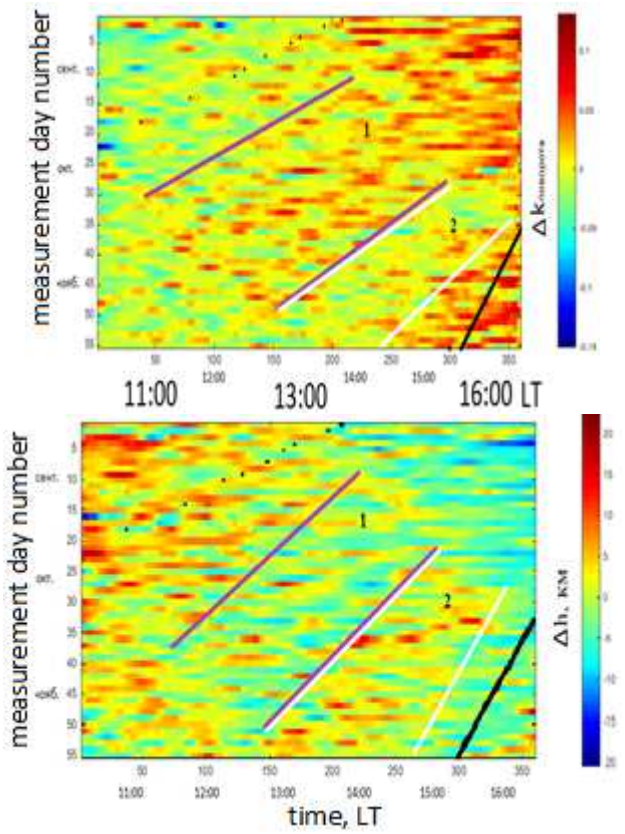

Figure 3. Seasonal-diurnal pattern of the occurrence of MS and SSTIDs by variations of $k_{US/DS}$ (top) and h_{PC} (bottom).

3 Conclusion

Thus, the use of a simple indicator of weak mid-latitude TID medium and small scales in ionograms was successful. This paves the way in the direction of studying their origin. So, not only tropospheric internal gravity waves (IGWs), or IGWs of auroral origin, but also electric fields of plasmospheric origin can have the appearance of regular weak TIDs.

4 Acknowledgements

The work is performed according to the Russian Government Program of Competitive Growth of Kazan Federal University.

5 References

1. R. O. Sherstyukov, A. D. Akchurin, O. N. Sherstyukov, “Collocated ionosonde and dense GPS/GLONASS network measurements of midlatitude MSTIDs,” *Advances in Space Research*, **61**, 2018, pp. 1717-1725, doi: 10.1016/j.asr.2017.11.026.

2. R. O. Sherstyukov, A. D. Akchurin, O.N. Sherstyukov, “The problem of selection the satellite-receiver lines-of-sight in the practice of the ionosphere GNSS-sensing for weak MSTIDs observing,” *2019 Russian Open Conference on Radio Wave Propagation Proceedings*, no. 8810187, Kazan, July 2019, pp. 94-97, doi: 10.1109/RWP.2019.8810187

3. F. T. Djuth, H. C. Carlson, L. D. Zhang, “Incoherent scatter radar studies of daytime plasma lines,” *Earth Moon Planets*, **121**, 1-2, 2018, pp. 13-43, doi: 10.1007/s11038-018-9513-5

4. G. Smirnov, A. Akchurin, “Comparison of electron densities and temperatures on satellite in situ measurements and ground remote observations,” *2019 Russian Open Conference on Radio Wave Propagation Proceedings*, no. 8810370, Kazan, July 2019, pp. 131-134. doi: 10.1109/RWP.2019.8810370

5. J. V. Evans, “Satellite beacon contributions to studies of the structure of the ionosphere,” *Reviews of Geophysics*, **15**, 3, 1977, pp. 325-350. doi:10.1029/RG015i003p00325.

6. K. Davies, “Recent progress in satellite radio beacon studies with particular emphasis on the ATS-6 radio beacon experiment,” *Space Science Reviews*, **25**, 4, pp. 357-430. doi: 10.1007/BF00241558.

7. E. L. Afraimovich, N. P. Perevalova, *GPS-monitoring of the Earth's upper atmosphere*, 2006, 480p., SC RRS SB RAMS, Irkutsk. (in Russian)

8. A. D. Akchurin, V. V. Bochkarev, V. R. Ildiryakov, K. M. Usupov, “TID selection and research of its characteristics on ionograms,” *Proc. of 30th URSI GASS 2011*, Istanbul, August 2011, no. 6050965, doi:10.1109/URSIGASS.2011.6050965

9. A. Akchurin, G. Smirnov, “MSTID extraction from more frequent ionograms,” *Proc. of 32nd URSI GASS*

2017, Montreal, August 2017, no. 8105046, doi: 10.23919/URSIGASS.2017.8105046.

10. J. A. Whalen, "The daytime F layer trough and its relation to ionospheric-magnetospheric convection," *Journal of Geophysical Research*, **94**, A12, 1989, pp. 17169-17184, doi: 10.1029/JA094iA12p17169.

11. J. C. Foster, "Cold plasma redistribution throughout geospace," *Science China Technological Sciences*, **59**, 9, 2016, pp. 1340-1345, doi: 10.1007/s11431-016-6047-9.

12. J. C. Foster, H. B. Vo, "Average characteristics and activity dependence of the subauroral polarization stream," *Journal of Geophysical Research*, **107**, A12, 2002, pp. 1475, doi:10.1029/2002JA009409.